EFFECT OF H-MORDENITE ZEOLITE AS A COMPONENT IN Co-Mo-Al_2O_3 HYDROPROCESSING CATALYSTS USED FOR THE CONVERSION OF BOSCAN HEAVY OIL

Rwaichi J.A. Minja and Marten Ternan
Synthetic Fuels Research Laboratory

ENERGY RESEARCH LABORATORIES
DIVISION REPORT ERL 89-77(J)

This work was supported in part by the Federal Panel on Energy Research Development (PERD)

EFFECT OF H-MORDENITE ZEOLITE AS A COMPONENT IN Co-Mo-Al_2O_3 HYDROPROCESSING CATALYSTS USED FOR THE CONVERSION OF BOSCAN HEAVY OIL

by

Rwaichi J.A. Minja and Marten Ternan
Energy Research Laboratories/CANMET
Energy, Mines and Resources Canada
Ottawa, Ontario
K1A 0G1
Canada

and

Department of Chemical Engineering
University of Ottawa
Ottawa, Ontario
K1N 6N5

ABSTRACT

The effect of H-mordenite zeolite as a component in Co-Mo-Al_2O_3 hydroprocessing catalysts has been studied. Catalysts containing up to 20% H-mordenite were used for hydrocracking Boscan heavy oil at 13.9 MPa. Although the acidic sites on the external surface of the zeolite crystals were expected to increase cracking reactions, little effect on conversion was observed. As the H-mordenite content of the catalyst increased the bulk density and the specific surface area of the catalysts decreased substantially. When the reaction results were expressed on the basis of constant residence time and constant catalyst surface area there was an increase in the reaction parameter with increasing H-mordenite content of the catalyst. It was also found that, coke deposition increased with the increasing H-mordenite content of the catalyst. These two observations suggest that H-mordenite caused an increase in the number of acidic sites in the catalyst. The results indicate that catalysts with H-mordenite would produce greater conversions than catalysts without H-mordenite if the extrudates could be prepared in such a way that the catalyst bulk density does not change when the H-mordenite is added.

INTRODUCTION

Several studies performed in our laboratory have been directed toward the development of improved catalysts for hydrocracking oil sands bitumen and heavy oil. In the present study, the effect of adding H-mordenite to a conventional type of hydroprocessing catalyst was investigated. Conventional hydroprocessing catalysts are supported on alumina which has predominately Lewis acid sites. In contrast H-mordenite has Bronsted acid sites. An enhancement in the acidity of the catalyst surface by H-mordenite was expected to enhance the cracking reactions[1]. The catalysts containing H-mordenite were evaluated by hydrocracking Boscan heavy oil at high pressure.

The general objective was to determine the effect of the H-mordenite zeolite on the catalyst properties. A more specific objective was to determine whether the H-mordenite crystals cause a beneficial effect on any of the hydrocracking reactions. Na-mordenite is known[2] to have pore openings of 0.67 - 0.7 nm. Although the pores in H-mordenite are larger[3], they are still much too small to admit the typical 4 nm molecules[4-7] found in Boscan heavy oil. Since the feedstock molecules are generally too large to enter the H-mordenite pores, any beneficial effect would have to be attributed to the reaction sites on the external surfaces of the H-mordenite crystals, rather than the reaction sites within the pore structure.

EXPERIMENTAL

The catalysts used in this study were prepared in five steps. In the first step, appropriate amounts of ammonium paramolybdate ($(NH_4)_6.MO_7O_{24}.4H_2O$) dissolved in aqueous ammonia solution (7.9 g 29 wt % ammonia in 43 mL of water), cobalt nitrate hexahydrate ($Co(NO_3)_2.6H_2O$) solution, distilled water, and a small amount of 70 wt % nitric acid (about 14 mL concentrated acid per 18.4 g of ammonium paramolybdate) were added to alpha alumina monohydrate powder (Continental Oil Company, 100 mass % Catapal SB) in a mixer. The chemicals were added in the order listed above, and mixed until the paste was homogeneous.

The H-mordenite component was prepared in the form of a paste by adding a hydrocarbon distillate oil (Table 1) to the H-mordenite zeolite. It was purchased from Imperial Oil (trade name, Zerice). The H-mordenite was purchased from Union Carbide (product number LZM8). The H-mordenite powder was placed in a beaker and the oil was added dropwise while mixing with a spatula until the paste was uniform. The amount of H-mordenite used was calculated on the basis of wt % H-mordenite required in the final catalyst. The ratio of oil to H-mordenite used was about 1.4 mL oil per gram of H-mordenite.

Catalyst preparation was completed by mixing the two pastes described above (the third step). The H-mordenite paste was added to alumina in a mixer and mixed until uniform. The oil was expected to keep the alumina paste from entering the H-mordenite pores and thereby prevent changing the H-mordenite. Extrudates were prepared from the combined paste in the fourth step.

A hand extruder similar to that employed by DeLasa and Mahay[8] was used. In this extruder a steel plate, which contained several circular holes, was located at the bottom of an empty steel cylinder that was mounted vertically. The combined paste was placed on top of the plate. A piston was moved down the cylinder, by a screw mechanism, until it contacted the paste and squeezed the extrudate through the holes in the plate. Lastly, the extrudates were dried at 110°C for about 10 h and calcined at 450°C for 4.5 h. A catalyst without H-mordenite was also prepared by following the above procedure but omitting steps 2 and 3.

All catalysts were characterized by mercury intrusion porosimetry. The catalyst characteristics are shown in Table 2. The aluminium, silicon, molybdenum, and cobalt concentrations were measured by inductive coupled plasma (ICP) spectroscopy. Catalysts were mixed with a lithium borate flux and fused at 1000°C for 1 h. Subsequently, the fused solid was dissolved in 5% nitric acid at 90°C for 1 h and the resulting solution was analyzed by ICP. The wt % zeolite in Table 2 was the amount measured during preparation.

The geometric characteristics of the catalysts are also shown in Table 2. They were determined by mercury intrusion porosimetry using a Micromeritics Autopore II 9220 porosimeter. The surface area, S_{pore}, was determined by assuming the pores were cylindrical. The median pore diameter, d_{pore}, is the diameter at which 50% of the pore volume, V_{pore}, had been filled with mercury.

A fixed bed tubular reactor having 155 mL volume and a length to diameter ratio of 12 was used. The experimental apparatus was

described in detail elsewhere[9]. The reactor has three heating zones to control the temperature and a preheating zone to preheat the heavy oil to 300°C. The reactor was filled completely with catalyst extrudates. The heavy oil feedstock and hydrogen were fed continuously into the bottom of the reactor. Each catalyst was evaluated at 13.9 MPa and 400°C and 450°C. A liquid hourly space velocity (LHSV) of 1.0 h^{-1} based on the total empty reactor volume was used in all cases. The hydrogen flowrate was set at 36.0 mL s^{-1} at STP (5000 scf H_2/bbl of heavy oil) for each experiment. The feedstock was Boscan heavy crude oil from Venezuela. Its properties are given in Table 3.

Each catalyst was presulphided at 400°C for 1 h before evaluating by flowing bitumen and hydrogen through the catalyst bed. Previous[10] studies showed that presulphiding with the feedstock was equivalent to using hydrogen sulphide. After presulphiding, a steady state was established at the new reaction temperature. All liquid samples were collected over a 2 h period then analyzed for sulphur, nitrogen and Micro Carbon Residue (MCR). The sulphur content was determined by X-ray flourescence using a Princeton Gamma-Tech Model 100 Chemical Analyzer. The nitrogen content was determined by using a Dohrmann N-100 total nitrogen analyzer. The ASTM D4530 Method for determining micro-carbon residue (MCR) was followed using an Alcor model MCRT analyzer.

RESULTS AND DISCUSSION

Figure 1 shows that, the conversions of sulphur, nitrogen, and MCR decrease slightly as the zeolite content of the catalyst increases. MCR is a measure of the tendency of a substance (crude oil feedstock or product) to form coke (carbonaceous residue). The conversion results suggest that the zeolite has decreased the catalytic activity of the catalyst. This is surprising, since the zeolite was expected to increase the surface acidity of the catalyst. It is known that surface acidity increases as a zeolite content of a catalyst increases[11-13]. It has also been reported that the zeolite increases the interaction between Ni and Mo through the formation of surface aggregates[14].

Figure 2 shows a substantial decrease in specific surface area of the catalyst as the H-mordenite content is increased, especially above 5 wt %. Possibly, the decreases in hydrodesulphurization (HDS), hydrodenitrogenation (HDN), and MCR removal, shown in Figure 1 are related to the loss in surface area available for the hydrocracking reactions.

To examine this a pseudo turnover frequency (PTOF) was calculated for each catalyst. The PTOF is defined as the number of S atoms (or N atoms) removed per second per nm^2 of surface area. It is expected to be related to the turnover frequency (TOF), which is the number of reactions per second per reaction site. Many heterogeneous catalysts have more than one type of reaction site. Each type of site is expected to have a different TOF. The PTOF provides an average turnover frequency for the different reaction sites on a unit of catalyst surface area.

The results in Figure 3 show that the PTOF increases with increasing H-mordenite content. However, one of the points (10 wt % H-mordenite) deviates from the curve. Nevertheless, this general trend in Figure 3 indicates that when the results are compared on a unit catalyst surface area basis, the mordenite component enhances the reactions.

A few laboratory studies have been performed in which zeolites were used in hydroprocessing[15-19]. In these studies the Bronsted acidity of the zeolites increased cracking and hydroconversion. A Ni/W/zeolite Y catalyst has been reported[16] to have a higher conversion to products boiling below 300°C than amorphous aluminosilicate-based catalyst ($Ni/W/SiO_2.Al_2O_3$). Sambi and Mann[19] reported that 25% zeolite was optimum for $NiO-MoO_3$ catalysts.

The molecules used in this study are much too large to enter the pores of H-mordenite. Therefore it is likely that the reaction sites on the external surfaces of the H-mordenite crystals are responsible for the beneficial effect shown in Figure 3. Gas oil molecules are also too large to enter the pores of the zeolites used in fluid catalytic cracking (FCC) catalysts. In this case the enhanced reaction rates are also attributed to reaction sites on the external surfaces of zeolite crystals[20].

Figures 4A and 4B show the mercury porosimetry curves for the catalyst with no H-mordenite and with 20 wt % H-mordenite respectively. Mercury porosimetry was used to determine the pore size distribution, median pore diameter, particle density and the specific pore surface area of the catalysts. At each pressure the curve at the lesser value of

mercury volume corresponds to mercury penetrating the pore, where as the curve at the greater value of mercury volume corresponds to mercury retracting from the pore. In all catalysts, the mercury could penetrate pores between 100 μm and 3 nm, at the pressures used with this equipment. From the mercury penetration curves, the pores can be divided into three regions of different sizes. The pore volumes in the regions of larger pores (d_p > 10 μm) medium pores (10 nm < d_p <10 μm), and smaller pores (d_p < 10 nm) are shown in Table 2. For each region the catalyst with 20 wt % H-mordenite (Figure 4B) has more pores than that with no H-mordenite (Figure 4A). The major difference between the two catalysts lies in the region of the medium pore range. The catalyst with 20 wt % H-mordenite has considerably more pore volume in this range. Although there is an increase in the volume of pores for the three regions discussed above, most of the pore volume in all cases is in the smaller range.

Figure 5A shows that the bulk density of the catalysts decreased as the H-mordenite content increased. The bulk density was obtained by measuring the weight of catalyst loaded into the 155 mL volume reactor. Thus, in addition to the decrease in specific surface area, there was also a decrease in the amount of catalyst. The 10 wt % H-mordenite catalyst is an exception. The combined decreases in these two features, i.e., specific surface area and the weight loaded in the reactor, as the H-mordenite increased, caused a large decrease in the total catalyst surface area in the reactor. This undoubtedly contributed to the decrease in the overall conversion shown in Figure 1. It should be noted that the data point for the 10 wt % H-mordenite catalyst deviates from both the line in Figure 3 and in Figure 5A.

The decrease in the catalyst bulk density with increasing H-mordenite content was partially caused by the change in shape of the catalyst particles. As the amount of H-mordenite in the catalyst increased, the cylindrical extrudate shapes became progressively rougher and particularly more curved in the longitudinal dimension. This caused a larger void between the catalyst extrudates during packing, hence less catalyst was loaded into the reactor.

The relative residence time of a molecule in the reactor was calculated from the void volume between the catalyst extrudates in the reactor. The space between the extrudates was calculated by dividing the catalyst weight in the reactor by the particle density of the extrudate given in Table 2. This value was subtracted from the total volume in the empty reactor to give the void volume in the reactor. Using the correlation of Reilly et al.[21] a liquid hold-up of approximately 94% was estimated. The void volume in the reactor was multiplied by the percent liquid hold-up to obtain the volume of liquid in the reactor. This was divided by the volumetric liquid feed rate (mass flow rate multipled by liquid density) to obtain the relative residence time. The value used for liquid density (0.78 g/mL) is typical of the average of the feedstock and liquid product densities at reaction conditions.

The relative residence times, shown in Figure 5B, increase with increasing H-mordenite content of the catalyst. In this case the 10 wt % H-mordinite catalyst also deviates from the curve. The increase in relative residence time is caused by the increase in space between the catalyst extrudates in the reactor which results from the curvature of

the extrudates mentioned earlier. The catalyst with 10 wt % H-mordenite seems to pack more compactly compared with the others. Since the nature of packing depends on the particle shape and size, the increase in space between the catalyst extrudates is probably an indication of the difference in shape of the catalyst extrudates with increasing H-mordenite content.

Figure 6 shows the increase in PTOF with increasing residence time. Of more interest here, is the 10 wt % H-mordenite catalyst (relative residence time = 26 min.) which is much closer to the curve than in Figures 3 and 5. Figure 6 suggests that the increase of PTOF might have been caused by the increase in residence time rather than an increase in catalyst acidic sites with greater H-mordenite content in the catalyst.

To eliminate the issue of residence time, the PTOF were divided by their corresponding residence times. In Figure 7, the PTOF per unit residence time increases with increasing H-mordenite content. This suggests that it is the H-mordenite content rather than just the residence time that causes the increase in PTOF. If the phenomenon could be explained solely by residence time, a horizontal line would have been obtained. The residence time appears to be a minor factor rather than a major controlling factor.

There is a modest increase in median pore diameter with catalyst H-mordenite content as shown in Table 2. The possible influence of diffusion was considered using the following equation[22]

$$D_{eff}/D_{bulk} = (1-\lambda)^2/(1+p\lambda) \quad (1)$$

where D_{eff} is the diffusivity of the molecules in the catalyst pores, D_{bulk} is the diffusivity in the bulk liquid, d_m is the molecular diameter, d_p is the pore diameter, $\lambda = d_m/d_p$, and p is a constant parameter. We considered measurements of molecular diameter by viscosity[4], neutron diffraction[5], membrane diffusivity[6] and X-ray diffraction[7]. Based on the above findings, it was decided to use a molecular diameter of 4 nm which is typical of values obtained by viscosity measurements. Using the pore diameters in Table 2, and d_m=4nm, the values of λ shown in Table 2 were calculated. Using these values of λ and P=2 (Kuwait asphaltenes[22]), the ratio D_{eff}/D_{bulk} was obtained from Equation 1.

If diffusion was controlling the reaction, PTOF would increase with increasing d_p, since D_{eff} would also increase with d_p. When d_p becomes sufficiently large so that diffusion no longer has an influence, PTOF will remain constant with increasing d_p. On this basis PTOF would increase with D_{eff}/D_{bulk} or alternatively increase and then level out if diffusion affected the reaction. Since the graph of PTOF versus D_{eff}/D_{bulk} did not have either of these shapes, it was concluded that the surface reaction, rather than diffusion, had the dominant influence on PTOF. This conclusion is consistent with the fact that the λ values in Table 2 do not change radically, and that previous data[22] show that D_{eff}/D_{bulk} has a comparatively small change over this range of λ values.

Figure 8 shows that the amount of carbon deposited on the catalyst increases with the H-mordenite content of the catalyst. It is possible that both the increase in the carbon deposition shown in Figure 8, and the increase in reaction shown in Figure 7 may be caused by the increased number of acidic sites in the catalyst that are located on the exterior surface of the H-mordenite crystals. The increase in acidic sites on zeolite catalysts used for hydrotreating coal distillates has been investigated[15]. In that study, HDS rates were greater with catalysts having an HY zeolite component than with non-zeolite catalysts. Other workers[11] have studied the increase in acid centers as a function of zeolite content. These results support the suggestion that the increase in PTOF in this study may be associated with an increase in acid sites located on the external surfaces of the H-mordenite crystals.

CONCLUSION

Initially it appeared that the H-mordenite had no effect on typical hydrocracking conversion reactions as indicated in Figure 1. However, the H-mordenite caused almost a 20% decrease in catalyst surface area and almost a 40% decrease in catalyst bulk density. Further observation showed that the change in bulk density was caused by an increasing curvature of the extrudate shapes as the catalyst content of H-mordenite increased. Presumably the rheological properties of the paste, from which the catalyst was made, were gradually altered as more and more H-mordenite was added. In any event the extrudate shapes definitely became more and more curved as the H-mordenite content of the catalyst increased. The decrease in catalyst bulk density was particularly important because it was responsible for a change in the residence time of the liquid phase molecules in the reactor. When the reaction results were compared on the basis of unit residence time (Figure 7), it was clear that the H-mordenite caused increased reaction. This was supported by the increase in carbon deposition on the catalyst with increasing H-mordenite content in the catalyst. Since both coke deposition and cracking are enhanced by acid sites, it was concluded that the acid sites on the external surfaces of the H-mordenite, could have an influence on the hydrocracking reactions. For future work, it would be desirable to make H-mordenite extrudates that are straight, rather than curved, so that the catalyst bulk density remains relatively large. With a straight extrudate geometry, it is expected that the beneficial effect of H-mordenite will be reflected in the total conversion results in spite of a decrease in catalyst specific surface area.

LITERATURE CITED

1. Decroocq, D.; "Catalytic Cracking of Heavy Petroleum Fractions"; Gulf (Houston) and Technip (Paris); 1984; pp. 16-23.

2. Bolton, A.P.; "Molecular Sieve Zeolites, in Experimental Methods in Catalytic Research"; vol. 2 (ed. R.B. Anderson); Academic Press, New York; 1976; pp. 21-23.

3. Ruthven, D.M.; "Principles of Adsorption and Adsorption Processes"; Wiley, New York; 1984; p. 16.

4. Kyriacou, K.C., Baltus, E.R. and Rahimi, P., Fuel, 1988, 67, 109-113.

5. Ravey, J.C., Ducouret, G. and Espinat, D.; Fuel; 1988; 67, 1560-1567.

6. Kyriacou, K.C., Sivaramakrishna, V.V., Baltus, E.R. and Rahimi, P., Fuel, 1988; 67; 15-18.

7. Speight, J.G., "The Chemistry and Technology of Petroleum", Marcel Dekker, New York, 1980, 202.

8. DeLasa, H.I. and Mahay, A.; Personal Communication.

9. Kelly, J.F. and Ternan, M.; Can J Chem Eng; 1979; 57; 726-730.

10. Ternan, M. and Whalley, M.J.; Can J Chem Eng; 1976; 54; 642-644.

11. Radchenko, E.D., Sergienko, S.A., Chukin, G.D., Voitekhov, A.A. and Perezhigina, I. Ya.I.; Chem Technol Fuels Oils (English translation); 1983; 19, No. 6., 262-266.

12. Barthomeuf, D.; "Acidic Catalysis with Zeolites" in Zeolites: Science and Technology (ed. Ribeiro, F., Rodriques, A.E., Rollmann, L.D. and Naccache, C.), Martinus Nijhoff, Dordrecht; 1983; 317.

13. Benesi, H.A., Cat J; 1967; 8, 368-374.

14. Sidelkovskaya, V.G., Suring, S.A., Chukin, G.D., Skarzov, I.I., Aliev, R.R., Nefedov, B.K. and Turivskaya, L.V.; Kinetics and Catalysis (English translation) 1988; 29, 448-453.

15. Kirchko, A.A., Meged', N.F., Khor'kova, N.N., Yulin, M.K., Galkina, A.A. and Mezhlumova, A.I.; Chem Technol Fuels Oils (English translation); 1982; 18, No. 6, 273-276.

16. Maxwell, I.E.; Catalysis Today; 1987; 1, 385-413

17. Vazquez, M.I., Escardino, A., and Aucejo, A.; Can J Chem Eng; 1988; 66, 313-318.

18. Vazquez, M.I., Escardino, A. and Aucejo, A., Ind Eng Chem Res; 1988; 27, 2039-2043.

19. Sambi, I.S. and Mann, R.S., Can J Chem Eng; 1989; 67, 337-343.

20. Wojciechowski, B.W. and Corma, A.; "Catalytic Cracking"; Marcel Dekker, New York; 1986, 80-82.

21. Reilly, I.G., Scott, D.S., De Bruijn, T., Jain, A. and Pisko, Z.J.; Can J Chem Eng; 1986; 64, 705-717.

22. Ternan, M.; Can J Chem Eng; 1987; 65, 244-249.

TABLE 1: Properties of Distillate Oil

Specific gravity at 15°C	0.889
Carbon (wt %)	86.3
Hydrogen (wt %)	13.3
Nitrogen (ng/μL)	85.8
Boiling range °C	245 - 553
Atomic H/C ratio	1.85

TABLE 2: Catalyst Specifications

	WT %					
H-mordenite	0	1	3	5	10	20
Chemical Analysis						
Al_2O_3	81.5	81.2	80.0	78.9	76.5	72.4
MoO_3	15.4	15.3	15.1	14.9	14.4	13.5
CoO	3.1	3.1	3.1	3.1	3.0	2.9
SiO_2	0.0	0.3	1.7	3.2	6.0	11.2
Mercury Porosimetry						
S_{pores} (m^2/g)	194	195	191	196	184	169
d_{pores} (nm)	5.3	6.7	7.3	7.5	8.0	8.4
$\lambda = d_m/d_p$	0.75	0.60	0.55	0.53	0.50	0.48
Total Pore Volume						
V_{pores} (mL/g)	0.33	0.44	0.45	0.47	0.45	0.42
Volume of Larger Pores						
dp> 10 μm (mL/g)	0.0248	0.0412	0.0364	0.0468	0.0458	0.0417
Volume of Medium Pores						
10μm > dp> 10 nm (mL/g)	0.0795	0.1536	0.1572	0.1649	0.1484	0.1472
Volume of Smaller Pores						
dp< 10 nm (mL/g)	0.2245	0.2408	0.2545	0.2590	0.2567	0.2319
Particle density (g/mL)	1.441	1.265	1.222	1.205	1.225	1.187

TABLE 3: Properties of Boscan Heavy Oil

Specific gravity at 15°C	1.002
Carbon (wt %)	81.8
Hydrogen (wt %)	10.4
Nitrogen (wt %)	0.64
Sulphur (wt %)	5.38
Pentane Insolubles (wt %)	20.1
Toluene Insolubles (wt %)	0.10
Ash (wt %)	0.22
+525 Residue (wt %)	54.6
Vanadium	1385 ppm
Nickel	107 ppm

FIGURE 1 Conversion (wt %) versus H-mordenite zeolite content (wt %) of the catalyst. Figure 1A sulphur, Figure 1B nitrogen and Figure 1C micro carbon residue. Solid circles are for experiments at 450°C and open circles for experiments at 400°C.

FIGURE 2 Specific Surface area (m^2/g) versus Catalyst H-mordenite zeolite content (wt %).

FIGURE 3 Pseudo turnover frequency (atoms S or N removed $(nm)^{-2}s^{-1}$) versus H-mordenite zeolite content (wt %) of the catalyst. Figure 3A sulphur and Figure 3B nitrogen. Solid circles are for the experiments at 450°C and open circles for experiments at 400°C.

FIGURE 4 Cumulative Mercury Intrusion Volume (mL/g) Vs catalyst pore diameter (μm). Figure 4A - a catalyst without H-mordenite and Figure 4B - a catalyst with 20 wt % H-mordenite.

FIGURE 5 Figure 5A - Catalyst bulk density (g/mL) versus H-mordenite content (wt %) of the catalyst. Figure 5B - apparent residence time in the reactor (min) versus H-mordenite content (wt %) of the catalyst.

FIGURE 6 Pseudo turnover frequency (atoms S or N removed $(nm)^{-2}s^{-1}$) versus apparent residence time in the reactor (min). Figure 6A - sulphur and Figure 6B - nitrogen. Solids circles are for experiments at 450°C and open circles for experiments at 400°C.

FIGURE 7 Pseudo turnover frequency per residence time (atoms S or N removed $(nm^{-2}s^{-1})$ versus H-mordenite content of the catalyst. Figure 7A - sulphur and Figure 7B - nitrogen. Solid circles are for experiments at 450°C and open circles for experiments at 400°C.

FIGURE 8 Amount of carbon deposited per unit surface area of the catalysts (mgC/m^2) versus catalyst H-mordenite content (wt %).

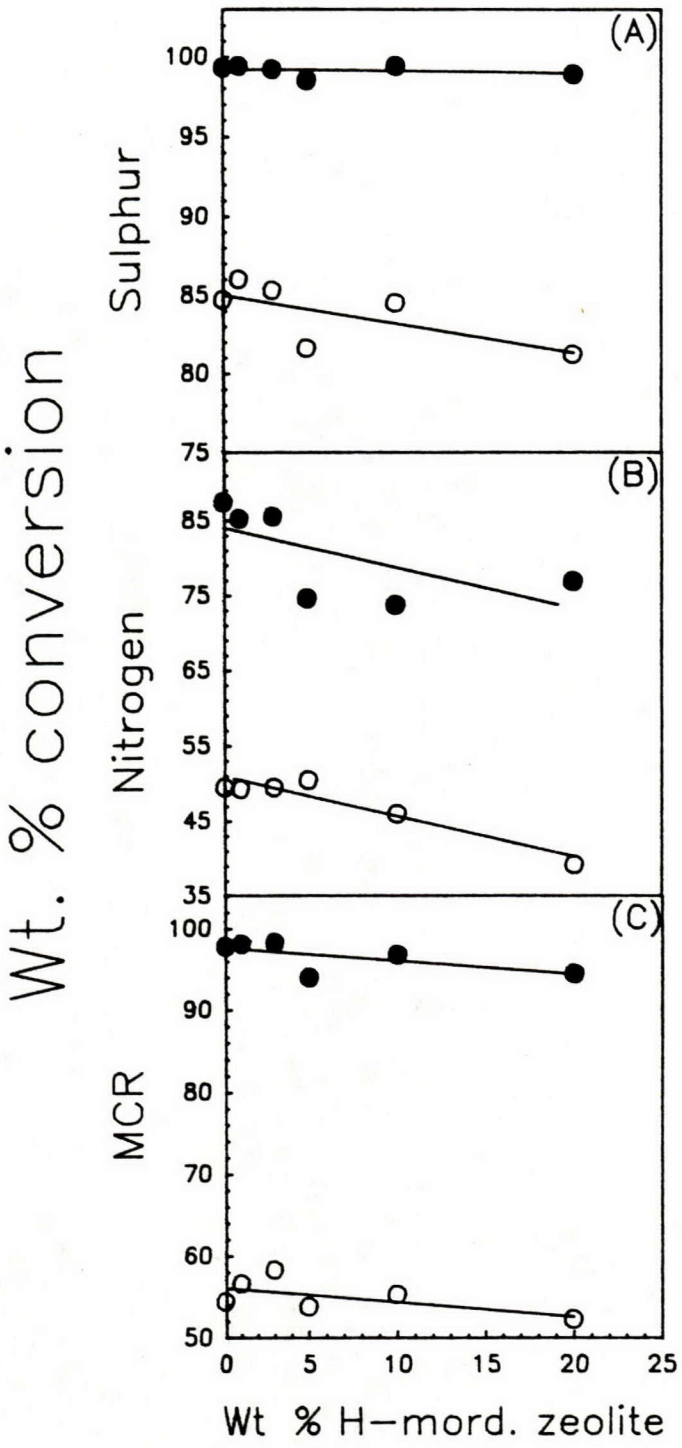
Wt. % conversion
Sulphur
Nitrogen
MCR
(A)
(B)
(C)
100
95
90
85
80
75
85
75
65
55
45
35
100
90
80
70
60
50
0
5
10
15
20
25
Wt % H—mord. zeolite

Figure 1

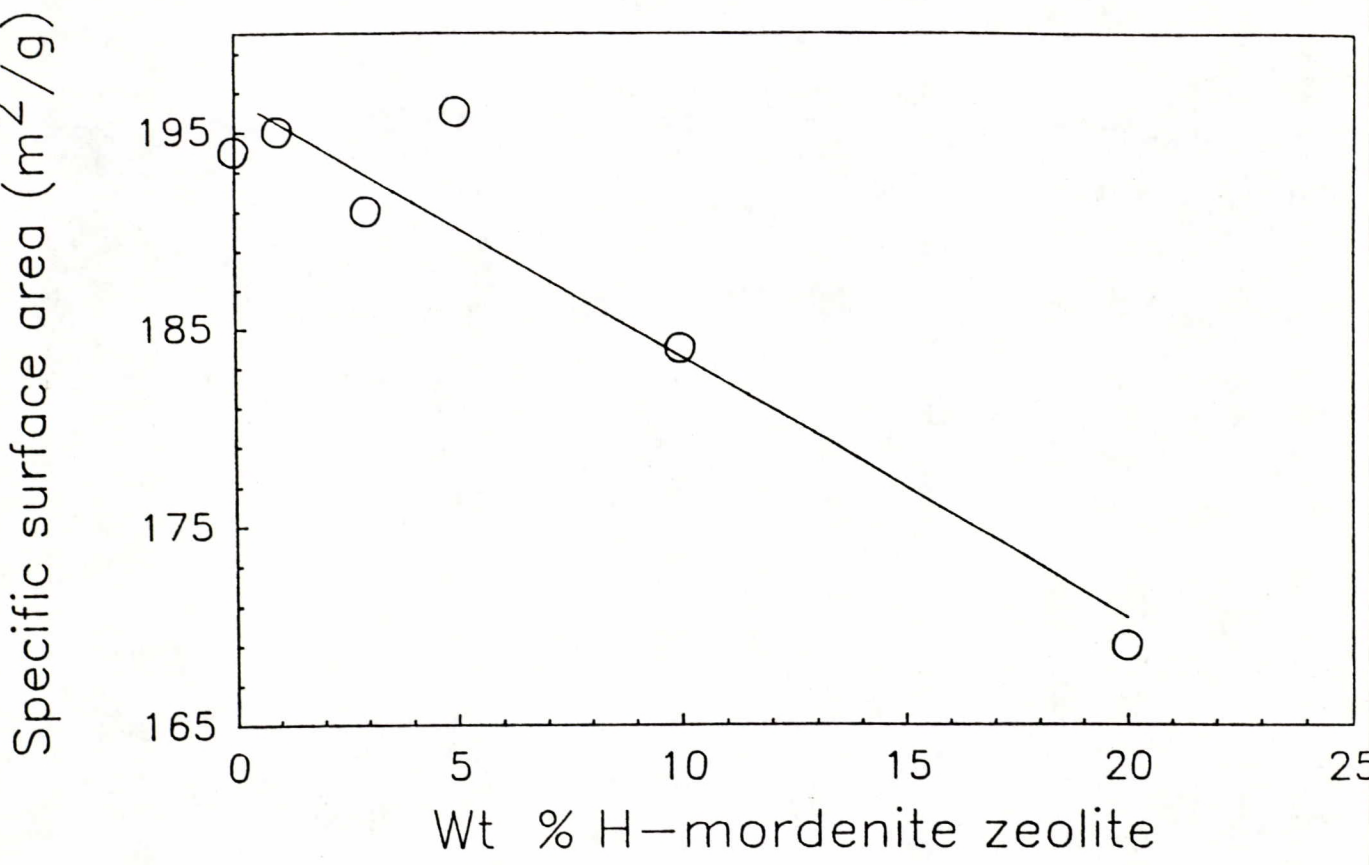
Specific surface area (m^2/g)
195
185
175
165
0
5
10
15
20
25
Wt % H−mordenite zeolite

Figure 2

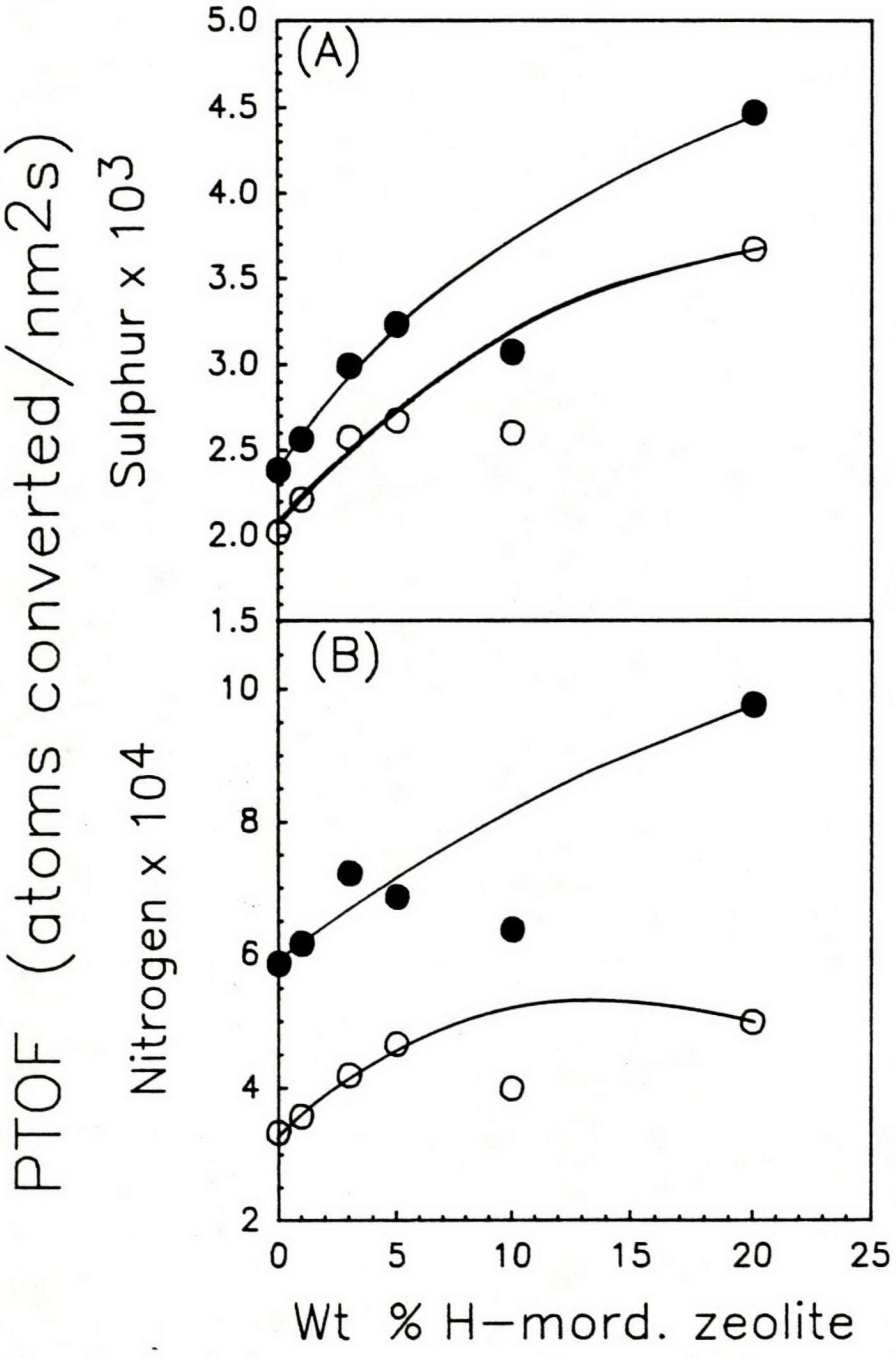
PTOF (atoms converted/nm2s)
Sulphur x 10^3
Nitrogen x 10^4
(A)
(B)
5.0
4.5
4.0
3.5
3.0
2.5
2.0
1.5
10
8
6
4
2
0
5
10
15
20
25
Wt % H-mord. zeolite

Figure 3

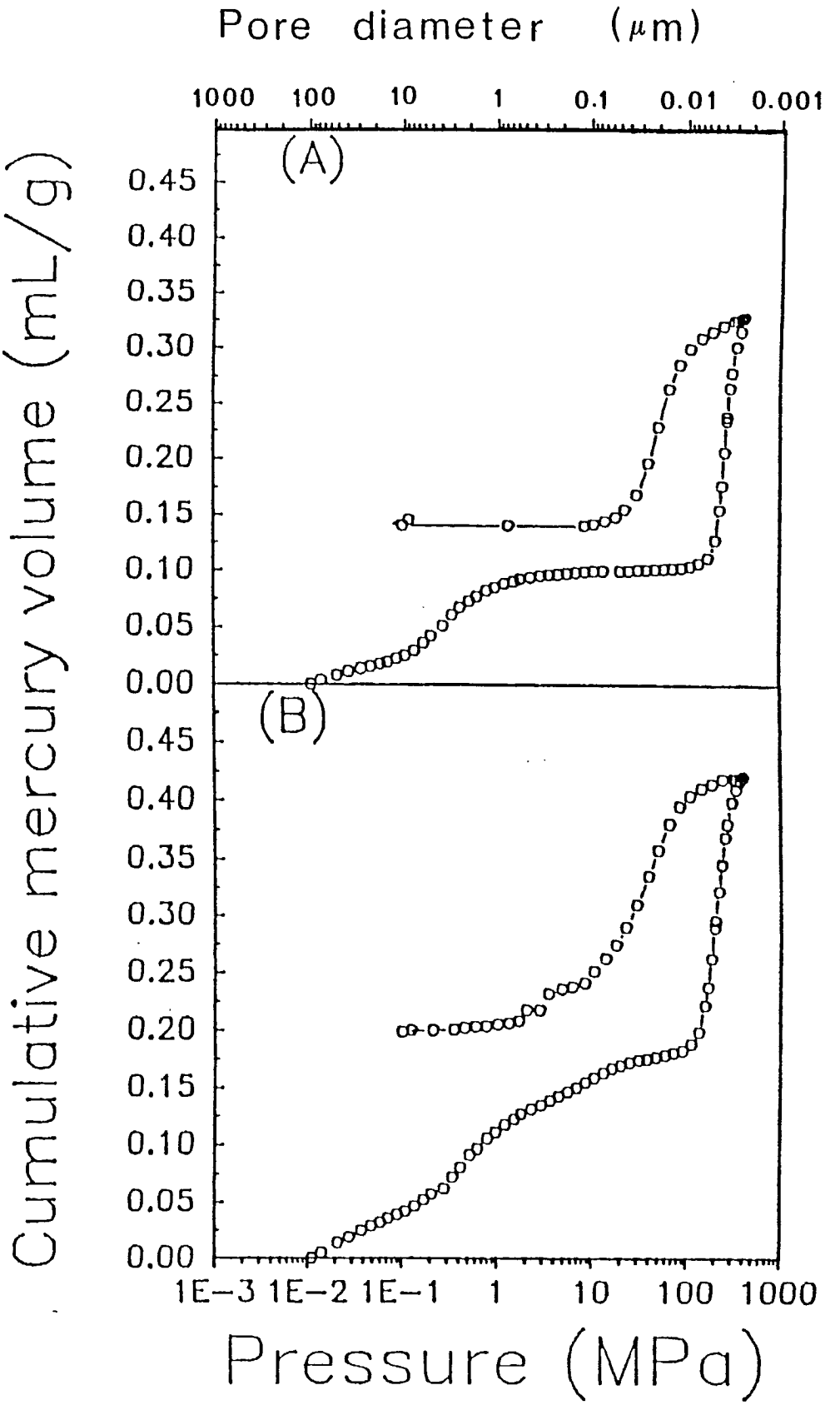
Pore diameter (μm)
1000
100
10
1
0.1
0.01
0.001
(A)
(B)
Cumulative mercury volume (mL/g)
0.45
0.40
0.35
0.30
0.25
0.20
0.15
0.10
0.05
0.00
1E-3
1E-2
1E-1
1
10
100
1000
Pressure (MPa)

Figure 4

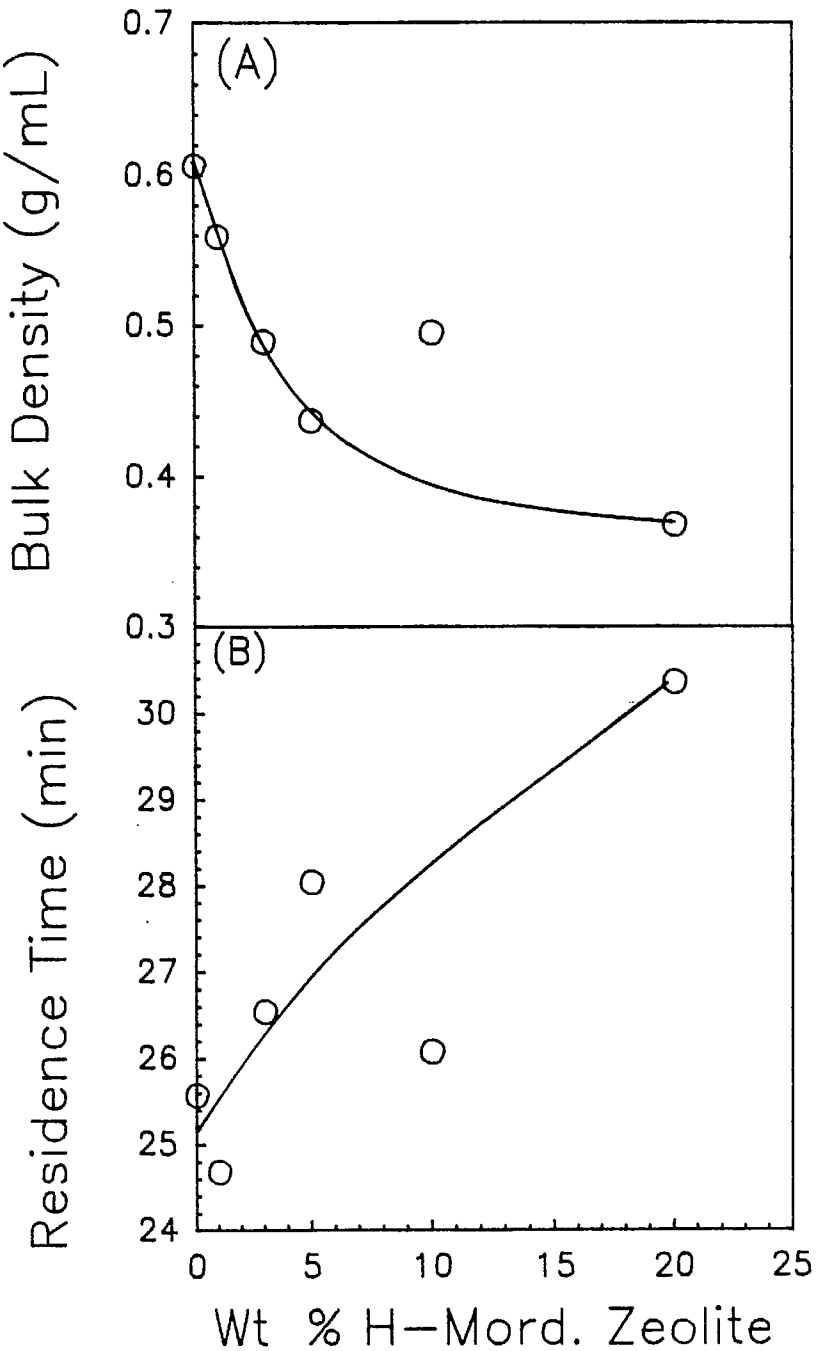
(A)
(B)
Bulk Density (g/mL)
Residence Time (min)
0.7
0.6
0.5
0.4
0.3
30
29
28
27
26
25
24
0
5
10
15
20
25
Wt % H-Mord. Zeolite

Figure 5

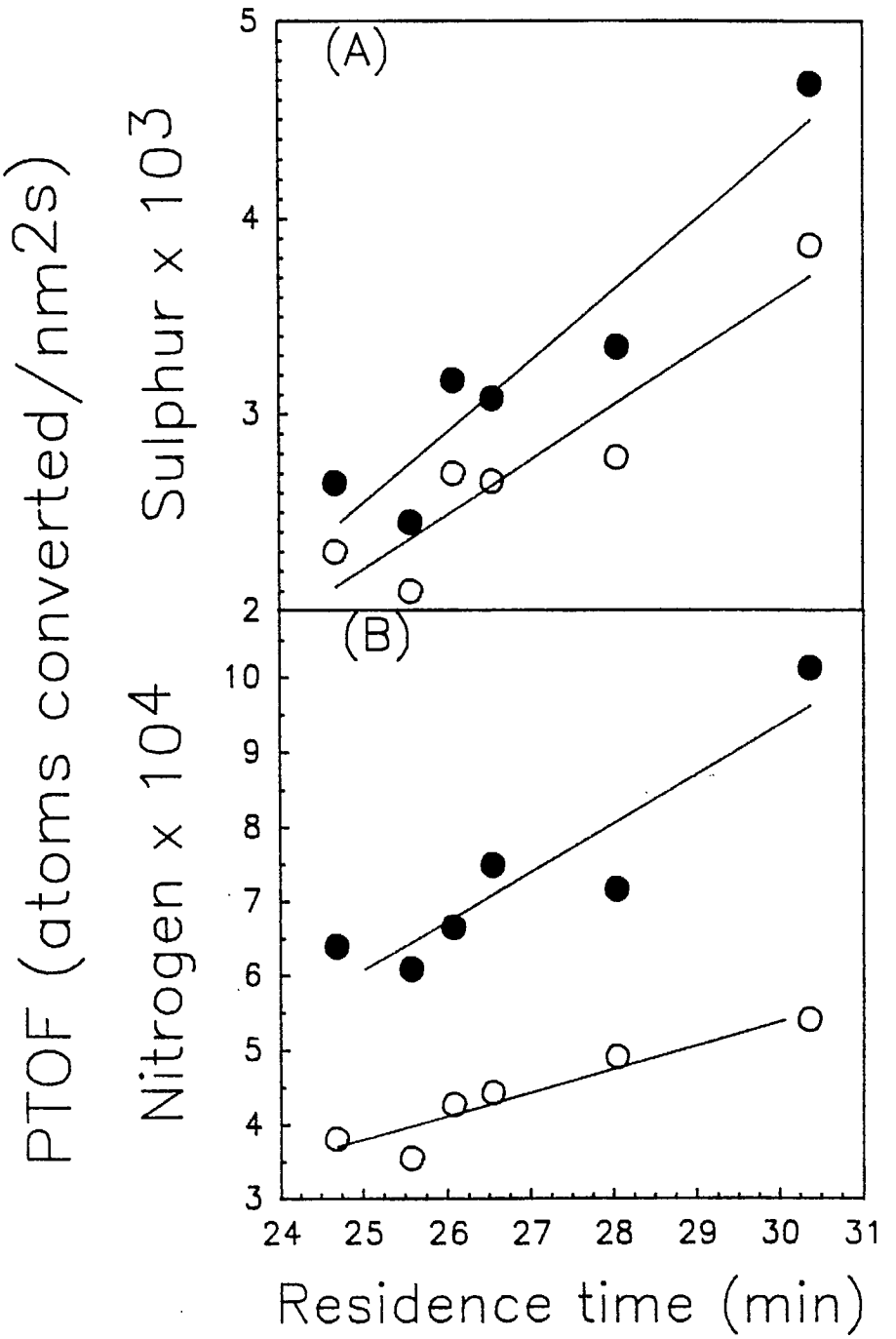
PTOF (atoms converted/nm2s)
Sulphur x 103
Nitrogen x 104
(A)
(B)
5
4
3
2
10
9
8
7
6
5
4
3
24
25
26
27
28
29
30
31
Residence time (min)

Figure 6

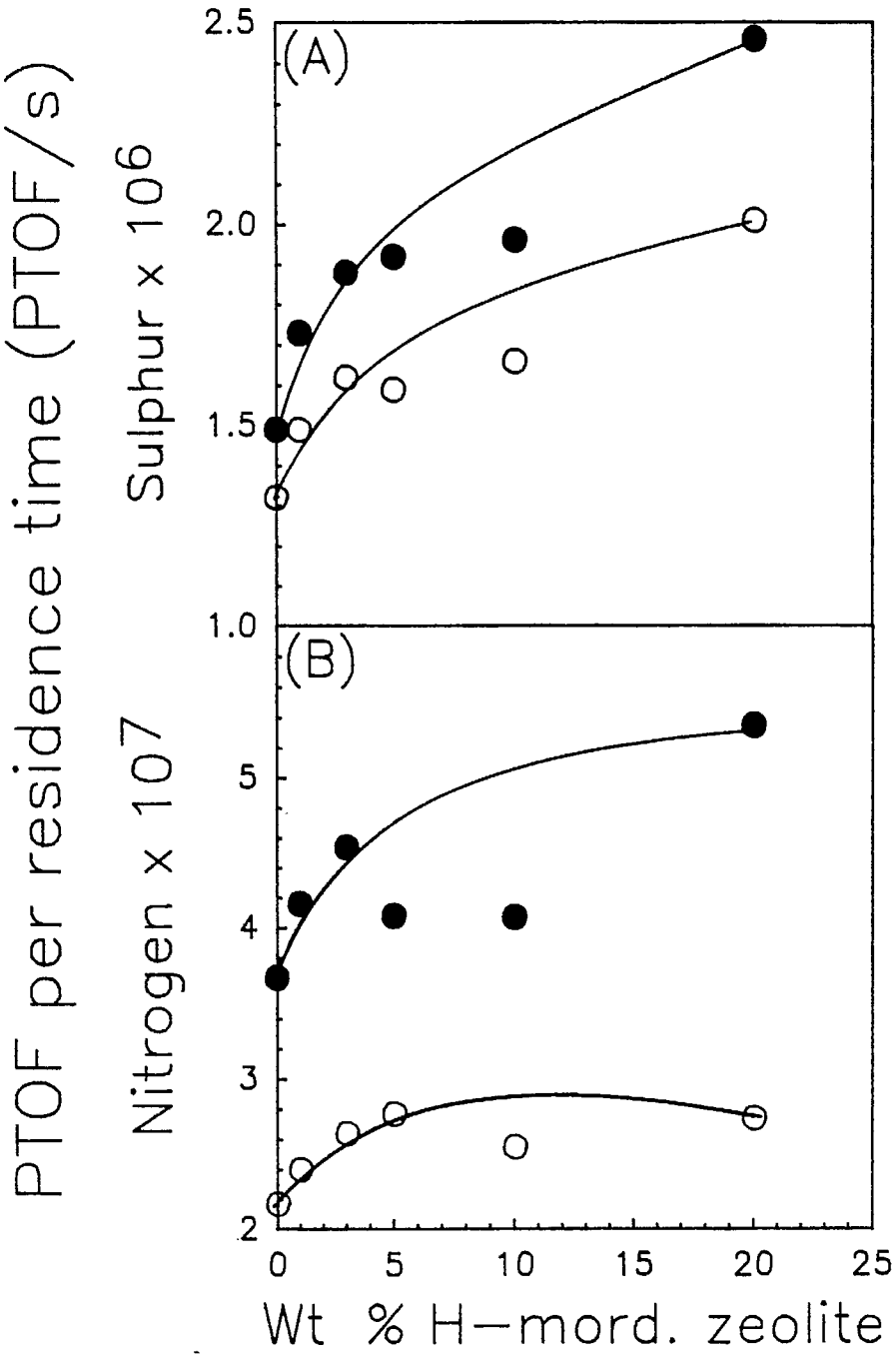
PTOF per residence time (PTOF/s)
Sulphur x 10^6
Nitrogen x 10^7
(A)
(B)
2.5
2.0
1.5
1.0
5
4
3
2
0
5
10
15
20
25
Wt % H—mord. zeolite

Figure 7

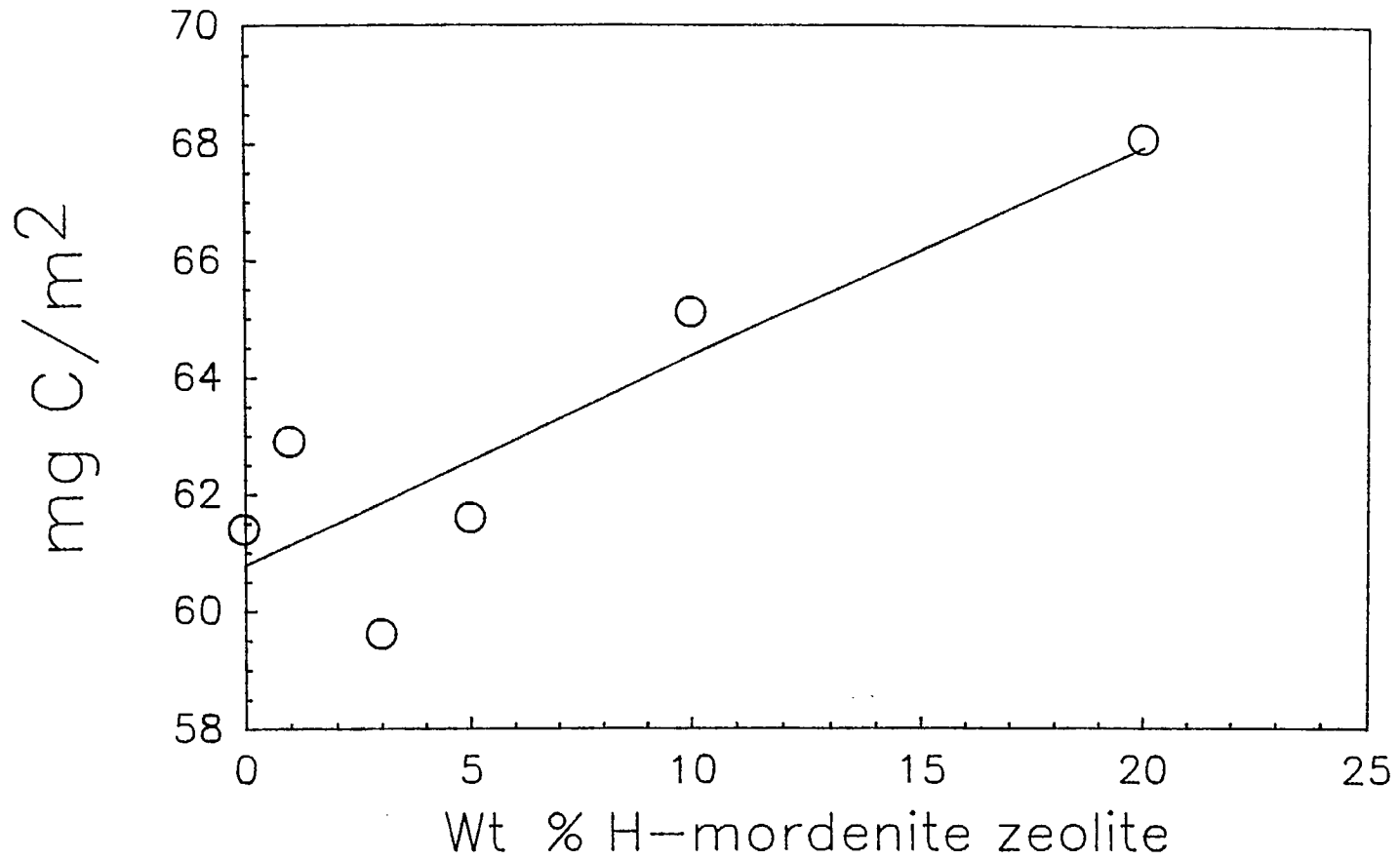

Figure 8